1999 Joint Meeting EFTF - IEEE IFCS

PERFORMANCE EVALUATION OF OPTOELECTRONIC OSCILLATORS.

S. Römisch, J. Kitching, E. Ferrè-Pikal#, L. Hollberg and F. L. Walls

National Institute of Standard and Technology, 325 Broadway, Boulder, CO 80303
#University of Wyoming, Laramie, WY

ABSTRACT

In the present work, we establish the importance of amplifier phase noise and system environmental fluctuations in determining the low-frequency ($f < 100$ Hz) noise of the oscillator. The system, designed to be a low phase noise microwave oscillator, has a measured single-side-band (SSB) phase noise of -123 dB/Hz (relative to 1 rad^2/Hz) at 10 kHz from the 10.6 GHz carrier. The fractional frequency stability required for advanced atomic frequency standards is on the order of $10^{-14}/\sqrt{\tau}$. This requirement might be met with an ideal version of this optoelectronic oscillator if we could reach the noise limit determined by the optical shot noise.

1. INTRODUCTION

The performance of a hybrid optical/electronic oscillator which uses a fiber-optic delay line as the frequency discriminator has been investigated and an evaluation of the possible use of this oscillator as a frequency reference for atomic standards has been done.

The traditional methods used to obtain spectrally pure microwave signals are based either on crystal oscillators (bulk-acoustic wave, BAW and surface acoustic wave, SAW) or on various schemes that utilize some sort of high-Q resonator (like whispering-gallery mode sapphire resonators). In the first case the output frequency needs to be multiplied, introducing signal degradation. In the second case the resonator requires more sophisticated technology than can usually be justified. A feature common to all such oscillators is the small tunability. This can be increased only at the expense of stability.

A promising alternative is the optoelectronic oscillator (OEO) that has been studied in several laboratories [1], [2], [3]. These hybrid opto-electronic systems use a long optical fiber as the selective element that permits high tunability and almost no limitation on the range of possible oscillation frequencies.

Furthermore, it is possible to define for the fiber a quality factor that defines its capability to select an oscillation frequency. This is similar to the Q factor used for resonators. In the fiber case, this factor is proportional to the product of the time delay introduced by the fiber and the oscillator's frequency. Recognition of this feature invites consideration of higher oscillation frequencies to improve the spectral purity the oscillation. The long delay also generates a high mode density and hence almost any oscillation frequency can be chosen.

Two undesirable features are the thermal dependence of fiber length, which limits the medium and long-term stability, and the non-negligible loss incurred in the conversion from microwave to optical and back again to microwave. To produce oscillation, this loss needs to be compensated, requiring microwave amplifiers that limit the medium-term stability due to their flicker phase noise.

A possible solution to the problem of amplifier phase noise is the use of two stages of amplification. The first amplifier would have low-power, low-flicker noise and the second would provide the remaining gain with its flicker noise canceled using the carrier suppression technique [4].

2. THE OPTOELECTRONIC OSCILLATOR

2.1 Basic scheme and equations

The general configuration for an OEO, shown in Fig. Figure 1, includes a CW laser, an electro-optic amplitude modulator (EOM), and a photodetector at the end of the optical fiber. The loop is then closed by an amplification stage, in order to reach the oscillation threshold, and some kind of filter which selects among the possible modes of this oscillator.

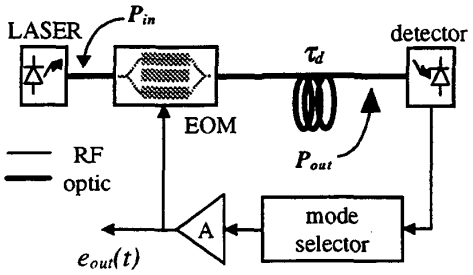

Figure 1. Basic scheme for an OEO.

In our system the EOM is a Mach-Zehnder type modulator which has a cosine-shaped transmittance versus drive voltage,

$$P_{out}(t) = P_{in}(t-\tau_d)\gamma\left[1+\varepsilon\cos\left(\pi\frac{V_{bias}+e_{out}(t-\tau_d)}{V_\pi}\right)\right], \quad (1)$$

where P_{in} and P_{out} are the optical powers incident on the modulator and detected at the end of the fiber. The modulator's parameters are γ, a factor related to the insertion loss; ε, a factor related to the extinction ratio and V_π, the bias voltage needed to move from a maximum to a minimum of the optical power transmitance.

The EOM is biased at the half-transmittance point so that the fundamental of the RF signal is transmitted to the detector. This signal is amplified and then fed back to the modulator. If the RF signal is written as

$$e_{out}(t) = V_0 \sin(\omega_0 t), \quad (2)$$

the oscillation condition will be set by

U.S. Government work not protected by U.S. copyright

$$P_{in}\gamma\left[1-2\varepsilon J_1\left(\frac{V_0\pi}{V_\pi}\right)\sin(\omega_0 t-\omega_0\tau_d)\right]=\frac{V_0}{A\rho}\sin(\omega_0 t), \quad (3)$$

where A is the gain of the RF amplifiers, ρ includes the detector responsivity and the fiber coupling loss, and $\omega_0=2\pi\nu_0$ is the oscillation angular frequency. The total delay along the loop is τ, the sum of the fiber delay τ_d and the much smaller delays of the others elements of the system (typically neglected here). The Bessel function comes from the series expansion of the transmittance the modulator.

The solutions of the oscillating term of Eq. (3) can be written as

$$\begin{cases} 2\gamma P_{in}\varepsilon J_1\left(\frac{V_0\pi}{V_\pi}\right)=\frac{V_0}{A\rho}, \\ \omega_0=\frac{(2K+1)\pi}{\tau_d}, \quad K=1,2,3\ldots . \end{cases} \quad (4)$$

The *mode selector* in Fig. Figure 1 selects a particular value of K (K=33 455 in our case) among all the solutions of Eq. (4).

In Eq. (3) and Eq. (4) the mode selector and the amplifiers are assumed to have a large enough bandwidth that the dynamics of the system are unaffected by them. A more detailed analysis of the oscillator can be found in [5].

2.2 Experimental arrangement

The experimental setup is shown in Fig. 2. The laser is an InGaAsP DFB device with a 3 mA threshold current and a maximum output optical power of 70 mW at a current of 200 mA. In our present experiments, a 100 mA current is used with an optical output power of about 35 mW. After passing through an isolator, the beam is coupled into the input fiber of the EOM. The inferred coupling efficiency is about 28 %.

The EOM has an insertion loss of about 3 dB and a V_π of about 6 V measured at the operating condition of the oscillator, that is, with a 10.6 GHz signal at the RF port. A servo system is needed to keep the bias point of the EOM stable. At this point (after the EOM) the remaining optical power is 7 % of the laser output power; the fiber coupling efficiency is 28 %, the passive insertion loss of the modulator is 50 % and another 50 % is lost due to the half-power bias point of the EOM.

The optical delay between the EOM and the detector is provided by a 1.2 km, single-mode, temperature-compensated optical fiber. This fiber has a temperature dependence of optical delay of 3 ps/(km·K) (compared to the typical fiber coefficient of about 30 ps/(km·K)).

In our present system the losses are significant and the photodetector sees only 5 % of the optical power delivered by the laser.

The detector is a commercial device with a bandwidth of 25 GHz and an inferred responsivity of 0.17 A/W. Although we are able to obtain (from the EOM) the maximum modulation depth (according to Eq. (3)) with the EOM input RF power near 22 dBm [22 dB (re 1 mW)], the detected RF signal is only -37 dBm as a result of losses primarily in the trasmission of the optical power. The total conversion loss from microwave to optical and back to microwave is about 62 dB.

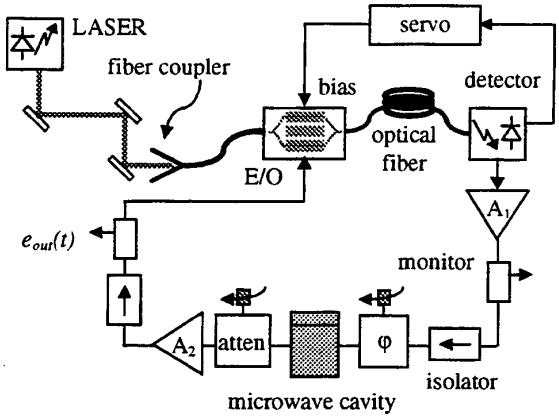

Figure 2. *Experimental setup for the opto-electronic oscillator (OEO).*

This number sets the minimum gain which needs to be provided by the RF amplifiers. A low-noise, high-gain amplifier provides the first 45 dB of gain and a low-noise, high-power amplifier provides the rest of the required gain and delivers the 22 dBm signal (3 dB compressed) to the RF modulator port.

The mode selector is between the two amplifier stages and is a critically coupled microwave cavity which introduces 6 dB of loss. Finally, the variable attenuator permits us to control the amount of compression in the system.

The resulting microwave signal shows a side-mode suppression of about 73 dB, due to the filter cavity with a loaded quality factor Q_L of about 8300.

3. THE NOISE

The phase noise of this oscillator can be at least partly predicted through a simple model described by Leeson, which has been adapted to this particular case [5]. In order to apply this model, we need to know the phase noise associated with each element of the system.

We therefore need to know the noise contribution of the detection process and the noise introduced by the amplification stages.

In our case the photodetector is simply terminated with a 50 Ω resistor, called R in the equivalent circuit of Fig. 3, where I_d is the noiseless photocurrent, containing both a DC and a RF component.

With an optical power of 1.75 mW (the 5 % of 35 mW delivered by the laser) incident on a detector with responsivity 0.17 A/W, the shot-noise is $\overline{i_{shot}^2}=2eI_d \cong -220$ dB/Hz. Then, the white phase noise delivered to the load, calculated from the circuit in Fig. 3 will be

$$S_\varphi(f)\Big|_{shot} = \frac{\overline{i_{shot}^2}\,R^2 R_L}{2P_{rf}\left(R+R_L\right)^2} = -145 \ \frac{\mathrm{dB_{rad}}}{\mathrm{Hz}},$$
$$S_\varphi(f)\Big|_{therm} = \frac{\overline{i_{therm}^2}\,R^2 R_L}{2P_{rf}\left(R+R_L\right)^2} = \frac{kT}{P_{rf}} = -140 \ \frac{\mathrm{dB_{rad}}}{\mathrm{Hz}}, \quad (5)$$

where P_{rf} is the signal power measured at the detector output (-37 dBm) and the dB_{rad}/Hz are intended relative to one squared radians. The term associated with the resistor's thermal noise is clearly dominant.

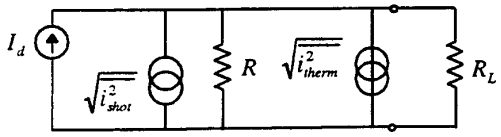

Figure 3. Photodetector equivalent circuit with shot noise and thermal noise sources. The load resistor is the input impedance of the first amplifier and is assumed to be 50 Ω.

The equivalent input phase noise of the amplifiers has been evaluated and includes all other RF devices except the cavity. This ensemble, called the *RF chain*, is displayed in Fig. 4, with the measurement results shown in Fig. 5.

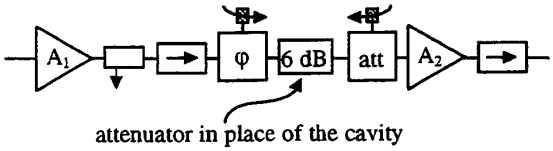

Figure 4. Elements considered in the RF chain.

The total phase noise at the input of the RF chain is the sum of the input equivalent noise of the RF chain and the white noise coming from the detection.

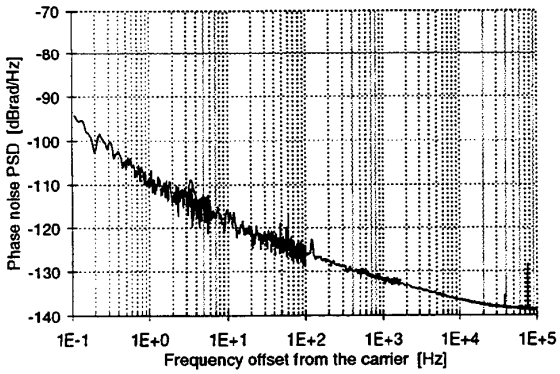

Figure 5. Phase noise power spectral density of the RF chain, *measured with an input signal power of -40 dBm at 10.571 GHz.*

These quantities can be used to predict the oscillator noise with the noise transfer function calculated according to the Leeson's model [5]:

$$S_\varphi(f)\Big|_{osc} = \frac{1}{\left(1-\cos(F(\Omega))\right)^2+\sin^2(F(\Omega))}\,S_\varphi(f)\Big|_{tot}, \quad (6)$$

with

$$F(\Omega) = \Omega\left(\tau_d + \frac{2Q_L}{\omega_0}\right), \quad (7)$$

where τ_d is the fiber delay. Q_L is the loaded quality factor of the microwave cavity, and $\Omega=2\pi f$ is the frequency offset from the carrier.

Fig. 6 compares the phase noise predicted by the model is compared to that measured with a frequency-discriminator noise-measurement system.

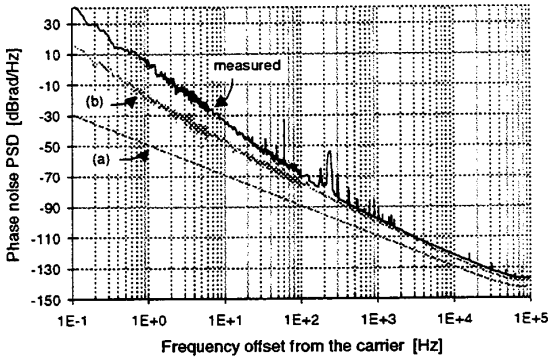

Figure 6. Measured and predicted phase noise PSD of the OPO. The noise predictions are made according to Leeson's model on the basis of the only white input noise (a) and the total equivalent input noise (b).

The measured data from Fig. 6 are replotted in Fig. 7 and analyzed in terms of power-law spectral densities. The small portion of white phase noise (slope f^0) around 100 kHz from the carrier is due to the presence of the first side-mode of the oscillator. For our 1.2 km fiber the free-spectral range is about 150 kHz and the side-mode suppression (with the present cavity) is only about 73 dB.

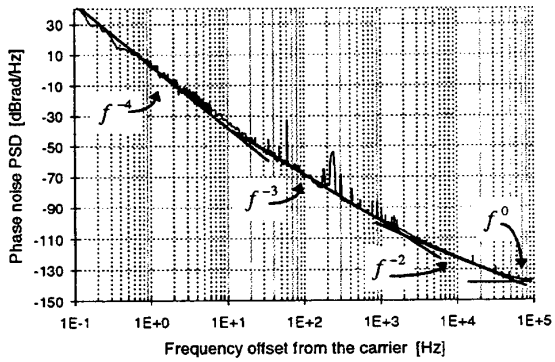

Figure 7. Measured PSD of the OPO with superposed power law model.

The next two segments with slope of 20 dB/decade and 30 dB/decade are due (as is clear from Fig. 6) to the white and flicker phase noise of the amplifiers.

The low-frequency part of the spectrum is random-walk frequency noise (slope f^{-1}) and is known to be mainly related to environmental factors such as temperature fluctuations and vibration.

4. PERFORMANCE EVALUATION AND FUTURE IMPROVEMENTS

One useful figure of merit for oscillators (even at different frequencies) is the Q-frequency product, which gives a general evaluation of the potential performance of the device. It is also possible to define a quality factor for a fiber that permits us to calculate our Q-frequency product [5] as

$$Q_{fiber} = \pi \nu_0 \tau_d, \qquad (8)$$

where ν_0 is the oscillator frequency and τ_d is the optical delay of the fiber. For this OEO we obtain about $2.2\ 10^{15}$ Hz while for the best quartz oscillators we have $1.6\ 10^{13}$ Hz in the case of a BAW and $1.05\ 10^{13}$ Hz for a SAW.

The important difference with respect to resonator-based oscillators is that in this case, the quality factor is proportional to the oscillation frequency. Since for this oscillator the Q-frequency product is proportional to ν_0^2, it is advantageous to have as high a working frequency as possible.

The actual measured frequency stability is shown in Fig. 8.

The flat part of the curve is due to the phase flicker noise in the loop (slope f^{-3} in Fig. 7) while the part with slope τ^{+1} is a direct consequence of the thermal drift of the fiber length.

If we calculate the Allan variance related to the asintote with slope f^{-2} of Fig. 7, we find $\sigma_y = 4.7\ 10^{-13}\tau^{-1/2}$ and, although this is an estimate that assumes the ability to remove all the excess low frequency noise, the oscillator is still not stable enough for use as a local oscillator for the new generation of atomic standards. For this OEO (ν_0=10.571 GHz), the white-frequency noise level (slope f^{-2} in Fig. 7) corresponding to a frequency stability of $\sigma_y = 10^{-14}\tau^{-1/2}$ is about -156 dBm/Hz at 10 kHz from the carrier. Since this portion of the noise spectrum comes from the open-loop white-phase noise, the simplest way to improve it is to obtain a higher RF signal at the detector output. That requires a higher detector responsivity and/or a higher laser power and a transimpedence amplifier photodetector.

However the low-frequency excess noise remains. In particular, the stability between 100 Hz and 10 kHz offset from the carrier is limited by amplifier flicker phase noise; a possible solution is to use a quieter first stage and carrier suppression techniques applied to the second stage. Finally, the medium and long-term stability of this oscillator is limited by environmental factors, and improvement will require temperature stabilization of the fiber.

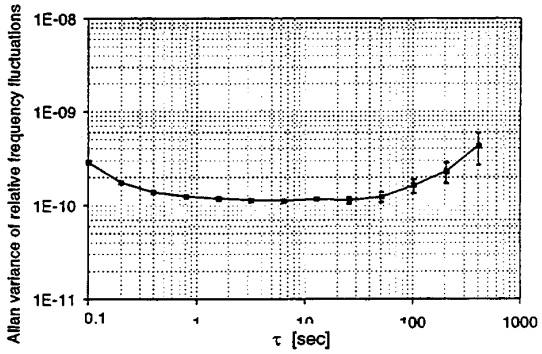

Figure 8. Allan variance of the relative frequency fluctuations versus integration time τ.

We thank S. R. Jefferts and F. Ascarrunz for many helpful and illuminating discussions. We are also grateful to R. Mirin and M. Young for a carefully reading of the manuscript.

5. REFERENCES

[1] X. S. Yao and L. Maleki, "High frequency optical subcarrier generator," Electron. Lett., Vol. 30, pp. 1525-1526, 1994.

[2] X. S. Yao and L. Maleki, "Optoelectronic oscillator for photonic system," IEEE J. Quant. Electron., Vol. 32, no. 7, pp. 1141-1149, 1996.

[3] J. Kitching, L. Hollberg, and F. L. Walls, "A 1 GHz optical-delay-line oscillator driven by a diode laser," in Proceedings of the IEEE International Frequency Control Symposium, 1996, pp. 807-814.

[4] E. N. Ivanov, M. E. Tobar and R. A. Woode, "Advanced phase noise suppression technique for next generation of ultra low noise microwave oscillator," in Proceedings of IEEE International Frequency Control Symposium, 1995, pp. 314-320.

[5] S. Römisch and A. De Marchi, "Noise predictions for the optoelectronic oscillator using different models," in these proceedings.

[6] X. S. Yao and L. Maleki, "New results with the opto-electronic oscillators (OEO)," in Proceedings of IEEE International Frequency Control Symposium, 1996, pp. 1219-1222.